Computational Study of Hydrogen Chemisorption on a Multi-Phenyl Organic Linker as a Model of Hydrogen Spillover on Metal-Organic Frameworks#

Sunghwan Choi, Kyeong-jun Jeong,‡ Ji Young Park, and Yoon Sup Lee*

*Department of Chemistry, KAIST, Daejeon 305-701, Korea. *E-mail: YoonSupLee@kaist.ac.kr*
Received September 28, 2014, Accepted November 30, 2014, Published online February 20, 2015

Hydrogen spillover reported on SNU-3 (empirical formula: $Zn_3C_{54}H_{60}N_2O_{18}$) is computationally studied to suggest viable mechanism for propagation of hydrogenation to the multi-phenyl organic linker and the proper organic linker for metal-organic frameworks (MOFs) with increased hydrogen spillover effect. Density functional theory calculations on the model compound of the linker indicate that, for the neutral organic linker, every aromaticity-breaking step to add hydrogen requires high energetic cost. For positively charged cases, the high endothermicity disappeared, facilitating hydrogen storage by spillover. Thus, hydrogen can be easily stored only for the positively charged linkers. It is also demonstrated that nitrogen-based organic linkers are more redox active than others, suggesting that MOFs that contain nitrogen-based organic linkers may be better hydrogen storage materials when the spillover is the primary mechanism in transition-metal-doped MOFs.

Keywords: Hydrogen spillover, Hydrogen storage, Metal-organic frameworks, Hydrogenation of phenyl compounds

Introduction

One of the recent topics in reversible hydrogen storage is hydrogen spillover, which is defined as dissociative chemisorption of hydrogen on a metal surface and subsequent migration of hydrogen atoms onto adjacent surfaces of a receptor via spillover and surface diffusion,[1] usually on metal-organic frameworks (MOFs). The interest in the hydrogen spillover is due to the possibility of increasing hydrogen storage capacity at room temperature.[2–4] To date, the storage ability of MOFs based on physisorption of hydrogen cannot satisfy all criteria that are accepted as standards for commercially successful storage materials. Especially, the inability to achieve room-temperature storage is the weakness of MOFs.[4–9] However, experiments have demonstrated that the hydrogen spillover can be utilized to achieve relatively efficient hydrogen storage at room temperature because the hydrogen atom may form a stronger bond to the host molecule than the hydrogen molecule. Moreover, experimentally, the reversibility problem, which usually plagues other chemical-bond-based media, does not appear in the hydrogen spillover on MOFs,[3,10,11] As the hydrogen spillover enhances the room-temperature storage and allows keeping strong points of typical porous materials, after Yang and his coworkers' pioneering work,[10,12–17] both experimental and computational reports have treated the topic.[18]

To date, hydrogen spillover phenomena have been reported on many different materials such as carbon nanotubes (CNTs),[19,20] activated carbon,[21,22] zeolites,[23] as well as MOFs including IRMOF-1,[10,24] IRMOF-8,[25,26] and MOF-177[27] in relation to hydrogen storage, but the phenomenon is a venerable subject in catalysis. Although the study of the hydrogen spillover effect on various materials will provide the opportunities to develop good substances for the storage, understanding hydrogen spillover on the atomic scale would be necessary to search and design appropriate storage materials efficiently. Classical hydrogen spillover phenomenon, based on 40 years of experimental results, was usually reported only on metal surfaces,[1] with the hydrogen atoms moving on the metal surface. Recent experiments on hydrogen spillover, however, were carried out as a strategy for hydrogen storage and involved the migration of hydrogen atoms from the metal surface to carbon-based surfaces. Even the additional migration from one carbon-based surface to another is included sometimes, and is called the secondary hydrogen spillover.

Both experimental and theoretical works have contributed to understanding the mechanism and predicting noble materials.[7–9,28–34] Lee *et al.*[6] studied a case of hydrogen spillover especially mediated by an electron hole on IRMOF-1, suggesting that the instability of the first intermediate state for hydrogenation of the organic linker of MOF disappears upon introducing an electron hole. Thus, the overall reaction, saturating benzene to cyclohexane, could be surmounted energetically. Additionally, the hydrogen atom bonded to the organic linker could move relatively easily to another site in the organic linker when the electron hole is formed. This strongly implies that the electron hole could play an important role in

This paper is dedicated to Professor Kwan Kim on the occasion of his honorable retirement.

‡ Present address: Department of Chemistry, University of Wisconsin-Madison, Madison, WI 53706, USA.

the hydrogen spillover process. Wu *et al*. reported that the hydrogen spillover on boron-substituted graphene could occur relatively easily.[35] They compared the reaction pathways corresponding to the migration of a hydrogen atom from the fully hydrogenated Pt_4 cluster on the bare graphene surface with that of boron-substituted graphenes. Based on the calculations on both migration and diffusion, the authors concluded that boron-substituted graphene could be a better material in terms of energy. Although Wu *et al*. did not refer to Lee *et al*. in the report, we think that boron-substituted graphene could show efficiency due to the creation of the effective electron–hole state in boron-substituted graphene.

Experimentally, an oxidized organic linker has not been reported in many MOFs. One of them was reported by Suh and Cheon on SNU-3 ($Zn_3C_{54}H_{60}N_2O_{18}$) by reducing Pd nanoparticles.[11] SNU-3 is one of MOFs that were synthesized in 2007 by the same group and whose organic linker is 4,4′,4″-nitrilotrisbenzoate (NTB).[36] NTB has a tertiary amine that is bonded to three phenyl groups. The authors reported that, when Pd nanoparticles are chemically generated, the tertiary amine is oxidized and becomes a radical. The radicals were detected by electron paramagnetic resonance spectroscopy. An increase in the hydrogen selectivity was reported and attributed to the spillover effect possibly induced by chemical doping. Considering reduction of the total void volume due to the blocked channel of MOF and the increase of total weight, it was also claimed that the amount of hydrogen adsorbed was dramatically increased, estimating that chemical doping enabled the MOF to contain 3.5 times more hydrogen than before. They concluded that this increase is most probably due to the hydrogen spillover made possible by Pd doping on SNU-3.

The hydrogen spillover effect on hydrogen storage materials is still controversial.[37] For example, it is not clear how the hydrogen atoms split by the catalyst migrate toward the other parts of the MOF. During the pathway from the catalyst particles to organic linker parts in the MOF, we can expect microscopic energy barriers that interrupt migration of hydrogen atoms. Due to the lack of clarity on that microscopic mechanism, we assume that hydrogen atoms are present near NTB, the organic linker of SNU-3. Then, we focus on thermodynamic stability of chemisorption of those hydrogen atoms on NTB, by interpreting the binding energies obtained from calculations.

In this article, we focus on the effect of the unpaired electron that is produced by an initial positive charge on NTB, and on the hydrogenation of the multi-phenyl organic linker. More specifically, we investigate how the hydrogenated phenyl makes the other connected phenyls to become a more easily hydrogenated system. Also, we show that the nitrogen-based organic linker of MOF can be redox-active, implying that many nitrogen-based organic linkers can be good spillover receptors in addition to NTB.

Computational Methods and Models

Optimization and frequency analysis were done by density functional theory (DFT) using the B3LYP functional as implemented in the GAUSSIAN 09 package.[38] All computations were performed with the 6-311++G* basis set. This level of computation has already been used in the previous hydrogen spillover studies.[39] To ensure accuracy, we discarded the results of highly spin-contaminated cases having S2 expectation values >10% larger than the exact value for the doublet (0.75) when we were examining open-shell systems.[25]

We terminated the organic linker of SNU-3 (NTB) with lithium atoms in order to reduce the size of the model to be explicitly calculated. NTB has three carboxylate functional groups originally bonded to zinc atoms, but we place lithium atoms near the tip of the carboxylate group to be at equidistant positions from two oxygen atoms (Figure 1(a)). This is one of the popular approaches when studying hydrogen spillover on MOF by the *ab initio* method.[6,25,28,32] Also, it has already been shown by other groups that including a zinc cluster in the computation does not induce a difference compared to the lithium-terminated model system. Hereafter, NTB without any comments refers to the model system that is terminated by Li atoms (see Figure 1(a)).

In order to discuss the dependence of adsorption energies on different carbon sites in the organic linkers, we need to refer to each carbon atom in different chemical environments. Chemically unique carbon atoms of NTB and BDC (benzene dicarboxylate, which is also lithium-terminated as NTB) were assigned the numbers following Figure 1(b) and (c) respectively. Unlike BDC, NTB has three phenyl rings in a molecule. We assign numbers to all three rings based on the imagined saturating order, although there is no difference between the phenyl groups in the initial NTB structure.

There can be many different ways of defining binding energies (or called adsorption energy). For example, binding energy is sometimes defined by referring the hydrogen atom

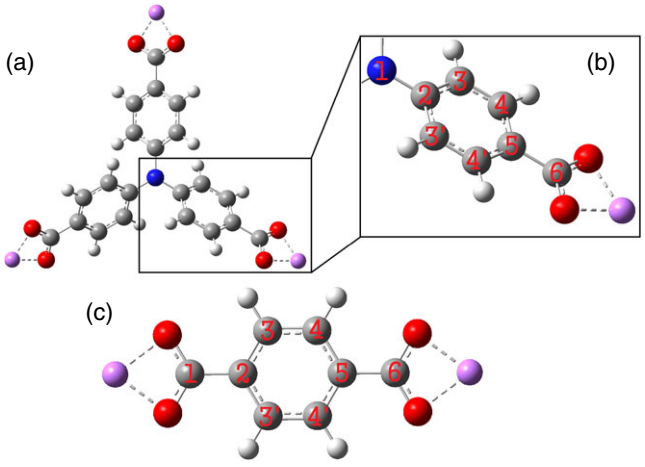

Figure 1. (a) Optimized structure of lithium-terminated NTB. (b) Site numbering on the phenyl ring on NTB. (c) Lithium-terminated BDC with numbering to identify sites. As in BDC, 3–4, 2–5, and 1–6 sites are chemically equivalent, hydrogenation energies of the sites in each pair are exactly same. Blue, gray, red, purple, and white balls represent nitrogen, carbon, oxygen, lithium, and hydrogen atoms, respectively.

state as the reference state; in other cases, it is defined relative to the hydrogen molecule as the reference state.[9,33] Here, we set the hydrogen molecule as the reference state and employ the binding energy per hydrogen molecule. Using this definition, we can easily compare the binding energy of this case with other hydrogen storage materials, and understand hydrogen spillover from a macroscopic viewpoint by defining two different energies, namely the average adsorption energy and the first hydrogenation energy. The average adsorption energy is defined as[6,12–17]

$$\Delta E_{av} = 2 \times \frac{[E(n\text{H@NTB}) - E(\text{NTB})]}{n} - E(\text{H}_2) \quad (1)$$

where E(NTB), $E(H_2)$, and $E(n$H@NTB) are the energies of the NTB, the hydrogen molecule, and the host molecule with n hydrogen atoms chemisorbed, respectively. The first hydrogenation energy is defined as

$$\Delta E_1 = 2 \times [E((n+1)\text{H@NTB}) - E(n\text{H@NTB})] - E(\text{H}_2) \quad (2)$$

where $E(n$H@NTB) and $E((n+1)$H@NTB) are the energies of the NTB chemisorbed by n hydrogen atoms on the first or the second ring and the same NTB having just one more hydrogen atom on another ring. Both ΔE_{av} and ΔE_1 imply the exothermic bonding to the host molecule when the value is negative.

Results and Discussion

Table 1 displays the first hydrogenation energies of NTB and BDC in order to show the consistency of the present scheme with other studies. The numbers in the first column are the site numbers assigned as shown in Figure 1. The second and the third columns refer to the present work. The data in third and fourth columns are from studies by Lee *et al.*[6] and Psofogiannakis *et al.*,[32] respectively. Although the first hydrogenation energies of BDC are computed by different levels of theory, the values show the consistency with each other, strongly suggesting that our choice of the computational scheme is reliable enough. That can imply that the computational accuracy on the NTB system may be acceptable as all calculations of BDC are quite similar despite the differences in the computational methods. It may be reasonable to assume that the current results for NTB would be reasonable in describing hydrogenated organic linkers.

Table 1. Calculated energy changes due to hydrogenation (kcal/mol).

	NTB	BDC		
Site \Method	B3LYP/6-311++G*[a]	B3LYP/6-311++G*[a]	B3LYP/6-311 + G**[b]	BP86/def2-TZVP[c]
1	122.7	119.2	109.6	125.7
2	63.2	57.8	59.8	61
3	50.9	48.4	46.4	47.2
4[d]	49.4	48.4	46.4	47.2
5[d]	59.5	57.8	59.8	61
6[d]	N.B.[e]	119.2	109.6	125.7

[a] This study.
[b] Lee *et al.*[6]
[c] Psofogiannakis *et al.*[32]
[d] In BDC cases, site numbers 4, 5, and 6 are same as 3, 2, and 1, respectively, because of the symmetry.
[e] No bonding.

Table 1 shows that the first hydrogenation on every position is highly endothermic. Among the six carbons on the phenyl group, the side carbons (the site 3, 4, 3′, and 4″ carbons in Figure 1) are the least endothermic in BDC. Even though the absolute values are slightly different, the first hydrogenation energy of NTB has the same tendency as BDC. One difference is that not all the side carbon atoms of NTB show equal ΔE_1 as the carbons on NTB are in a chemically different environment. The other tendency shared by both NTB and BDC is that the sites 1, 2, and 3 are less stable than 4, 5, and 6, respectively. Comparing the changing behavior of the hydrogenation energy of both molecules in terms of sites, the first hydrogenation energy values depended more on the closeness to the site 6, while the existence of nitrogen atom induced a relatively small difference. It implies that the first hydrogenation energy is strongly related to the characteristics of the phenyl group. The hydrogenation on the nitrogen site necessarily introduces the large increase in steric hindrance among three phenyl groups, and similar and smaller effects are in play to make hydrogenation energy larger for 2 and 5 carbon sites compared with 3 and 4 carbon sites. The small differences between 2 and 5 or 3 and 4 sites are mainly due to the electronegativity difference of N in site 1 and C in site 6.

Figure 2 shows the relationship between the number of hydrogen atoms attached to the first phenyl ring and the

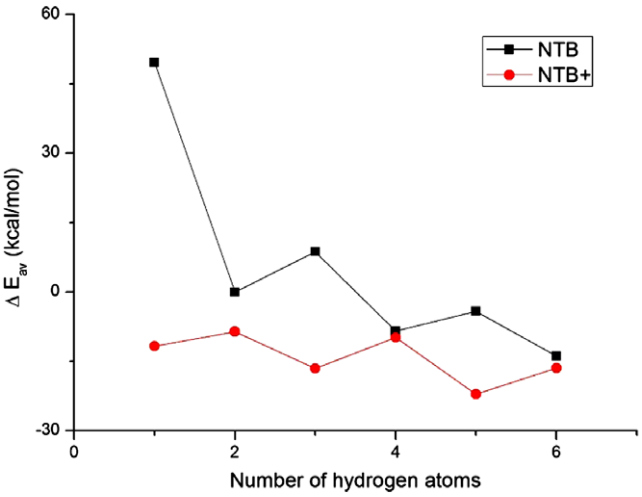

Figure 2. Energy change for the consecutive hydrogenation in a phenyl group of NTB, which is used as a model of SNU-3. Number of hydrogen atoms 1 refers to the first hydrogenation and 2 to the second hydrogenation, and so on.

average adsorption energies. As there are many combinations of sites to select from for a given degree of hydrogenation, we calculated all possible combinations and conformations to locate the most stable state. It was demonstrated in the SNU-3 system that the first step, which breaks the aromaticity of a phenyl group, is the unique endothermic step in the saturating process for the neutral system. That endothermic barrier is removed when NTB is positively charged. In both neutral and positively charged cases, two important trends are observed. The first one is that, for more hydrogen atoms attached to NTB, the newly formed bond induces larger energy changes. As the ring's aromaticity is broken by hydrogen attachment, the saturation process is more preferred thermodynamically. The second trend is that the closed-shell systems are more stable than open-shell systems, in line with the expectation that radicals are unstable. In neutral systems, even numbers of hydrogen atoms make ΔE_{av} lower, and, in positively charged systems, odd numbers of hydrogen atoms make ΔE_{av} lower. The reactivity of the radical is the reason why a positive charge makes the first step exothermic, instead of endothermic. In contrast to the neutral system, the positively charged system (NTB^+) is originally a radical. Accordingly, the first hydrogenation step could reduce the radical character of NTB^+ when it combines with the hydrogen atom. Another reason is that the positively charged system has resonance structures whose phenyl group does not possess aromaticity. In those resonance structures, the unpaired electron located on the radical moves to the beta carbons of the phenyl group. Hence, the carbons, which now have partially radical character, become preferred sites of hydrogenation.

In order to understand how adsorption energies change when more than one ring participate in hydrogenation, we calculated the first hydrogenation energy on a phenyl ring for systems that contain partially hydrogenated phenyl groups. As there are many possibilities involving two- or three-ring cases, we investigated only the first step of the saturation procedure. Hereafter, what is referred to as the two-ring saturation case is where one of three rings (called the first ring) is multiply hydrogenated and another ring (called the second ring) is subject to the first hydrogenation. In the two-ring saturation process, the third ring remains in its original phenyl form. In the same manner, what is referred to as the three-ring saturation case is where one of three rings (the first ring) is fully saturated by six hydrogen atoms, another ring called the second ring is multiply hydrogenated, and the third ring undergoes the first hydrogenation.

All ΔE_1 values of the two-ring saturation cases are summarized in Figure 3(a). In neutral NTB, all ΔE_1 values are about 50 kcal/mol, which is almost same as the first hydrogenation energy of the neutral NTB in Figure 2. When the second ring starts getting hydrogenated, the first step will take ~50 kcal/mol, which is energetically unfavorable. It implies that in neutral NTB the energy barrier of the aromaticity-breaking step is not related to hydrogenation of a connected phenyl group. Interestingly, when even numbers of hydrogen atoms are already attached to the first ring of NTB^+, the first hydrogenation energy of the second ring becomes significantly lower than that of the neutral NTB. With an odd number of hydrogen atoms attached on the first ring, the first hydrogenation energies of the positively charged system are also similar to the first hydrogenation energy of the neutral NTB case. This alternation of the hydrogenation energy for the charged NTB can be also explained by the radical character of the partially hydrogenated system. Either the reactant or the product of the first hydrogenation of the second ring should be a radical because the total number of electrons increases by one at every hydrogenation step. Within the even or odd numbers of hydrogen atoms on the first ring, the first hydrogenation energy of the second ring decreases as the number of hydrogen atoms on the first ring increases. This appears to imply that the first hydrogenation on the second ring will occur

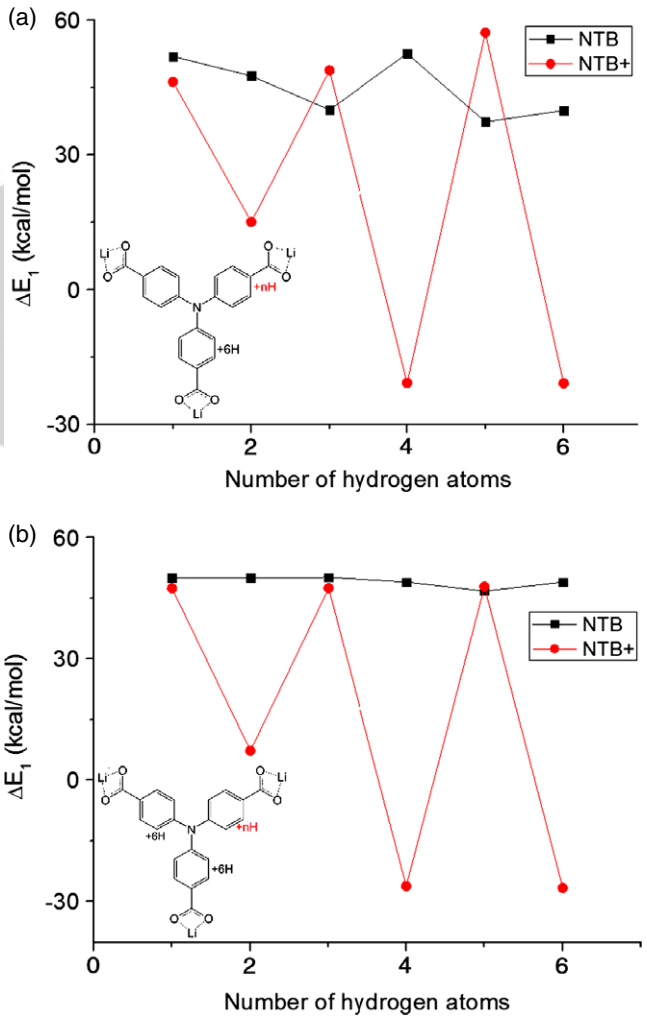

Figure 3. (a) First hydrogenation energy of the second phenyl group of NTB, with respect to the number of hydrogen atoms already attached to the first phenyl group when the third phenyl group is not hydrogenated. (b) First hydrogenation energy of the third phenyl group of NTB, with respect to the number of hydrogen atoms already attached to the second phenyl group. In this case, we let the first phenyl group saturated.

after the first ring is fully saturated for the positively charged NTB.

We also investigated the first hydrogen energies when hydrogenation on all three rings is in progress simultaneously. As two phenyl rings could change their degree of hydrogenation, an unmanageable numbers of possibilities are involved for this three-ring saturation case. Similar to the calculation in Figure 3(a), we optimized NTB systems that contain one fully saturated ring and one partially hydrogenated ring to examine only the first hydrogenation energy of the third ring, with respect to the extent of hydrogenation in the partially hydrogenated ring. Then the difference between the two-ring cases and the three-ring cases is whether one of the rings is a phenyl or a cyclohexane, which can be regarded as a fully saturated phenyl ring. Figure 3(b) shows the first hydrogenation energy of the third ring, which displays essentially the same pattern as the two-ring cases in Figure 3(a). Due to the flexibility of the cyclohexane group compared to the rigid phenyl group, hydrogenated NTBs may be optimized to slightly more stable structures. This could induce the binding energy values of neutral NTB to oscillate and decline as shown in Figure 3(b).

Figure 3(a) and (b) show that breaking pristine aromaticity can occur without high energy costs when the number of attached hydrogen atoms on adjacent phenyl groups reaches an even number. The first hydrogenation step cannot avoid overcoming the high energy barrier in the neutral NTB. If hydrogen is attached to one of the three rings, all subsequent steps of the hydrogenation process of the positively charged NTB become much easier than the ordinary hydrogenation step. However, on the uncharged NTB, there is no such stabilization effect.

In Figure 4, the red and black lines show atomic charge of the nitrogen center in the two- and three-ring cases, respectively, when NTB contains a positive charge. Blue dotted line corresponds to the atomic charge of nitrogen on the original

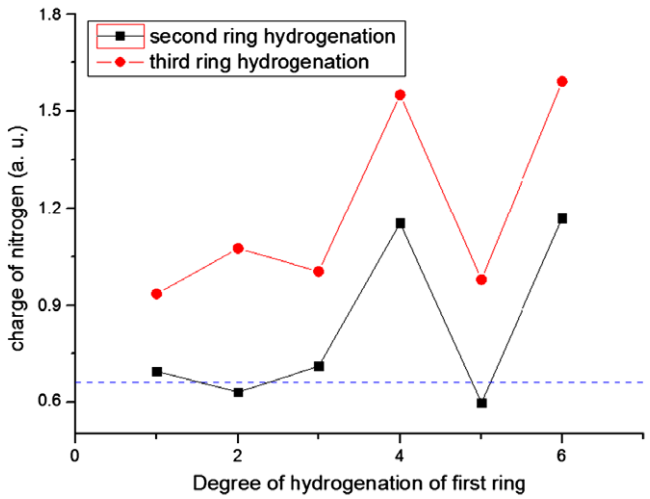

Figure 4. Atomic charges of nitrogen in hydrogenated NTB^+. The blue dotted line shows the atomic charge of nitrogen in pristine NTB^+.

NTB^+ without any attached hydrogen. All data are from the Mulliken charge population analysis. Blue line is located at about ~0.65, supporting that the positive charge is highly delocalized. When four and six hydrogen atoms attach to phenyl rings, nitrogen becomes dramatically positive compared to other cases. Those hydrogenation numbers correspond to those that facilitate the first hydrogenation of other rings. When the number of hydrogen atoms on the phenyl rings is even, closed-shell configurations are favored and radical characters are avoided. Alternatively, the phenyl ring with the odd number of hydrogen atoms attached is a radical, and the process to make two radicals disappear causes localized charges to be dispersed. However, when the hydrogenated phenyl itself completes the filling of the orbital, the charge on the nitrogen atom remains localized on nitrogen. It means that nitrogen contains the radical character which can be removed by the additional electron. By pairing electrons, positive charge on nitrogen could be diffused to other parts of the organic linker. As a result, the atomic charge becomes dramatically reduced when the degree of hydrogenation is over 4. Breaking the aromaticity of another phenyl ring may induce another electron to move to the center nitrogen, and the energy cost of breaking aromaticity could be compensated by forming another conjugation.

For IRMOF-1, it has been theoretically suggested that the organic linker becomes a good receptor for hydrogen spillover when positively charged.[6] However, there has been no experimental report of the positively charged BDC, which is the organic linker of IRMOF-1. In order to make the organic linkers of MOFs positively charged, Lee *et al.*[6] suggested defects in the metal cluster of MOFs, but the defects could lead to a serious decrease in the stability of MOFs. The other way to make an organic linker of the MOFs positively charged is to use chemical doping. It was reported that organic linkers play the role of a reducing agent.[11] Ionization energies are important criteria for organic linkers to be oxidized, and we calculated those for some organic linkers by observing the energy difference between optimized structures of neutral and positively charged organic linker molecules. Figure 5 contains the ionization energies of acetylenedicarboxylate (ADC), benzene-dicarboxylate (BDC), benzene-tricarboxylate(BTC), naphthalene-2,6-dicarboxylate(2,6-NDC), naphthalene-1,4-dicarboxylate(1,4-NDC), NTB, 1,3,5-benzene-tribenzoate (BTB) and *N*,*N*,*N*′,*N*′-tetrakis(4-carboxyphenyl)-biphenyl-4,4′-diamine (TCPDA). The organic linkers in Figure 5 are ordered according to the number of their phenyl groups. The structure optimizations of both neutral and positively charged linkers are performed with the same computational methods except for TCPDA; the ionization energy of TCPDA is a vertical ionization energy. The adiabatic ionization energy would be slightly smaller than one in Figure 5 for TCPDA.

The organic linkers can be classified into two types: one type is a set of organic linkers without a lone pair, and the other set is those with lone pairs. NTB and TCPDA belong to the second type, and other organic linkers in Figure 5 belong to the first. Figure 5 shows that increasing number of phenyl

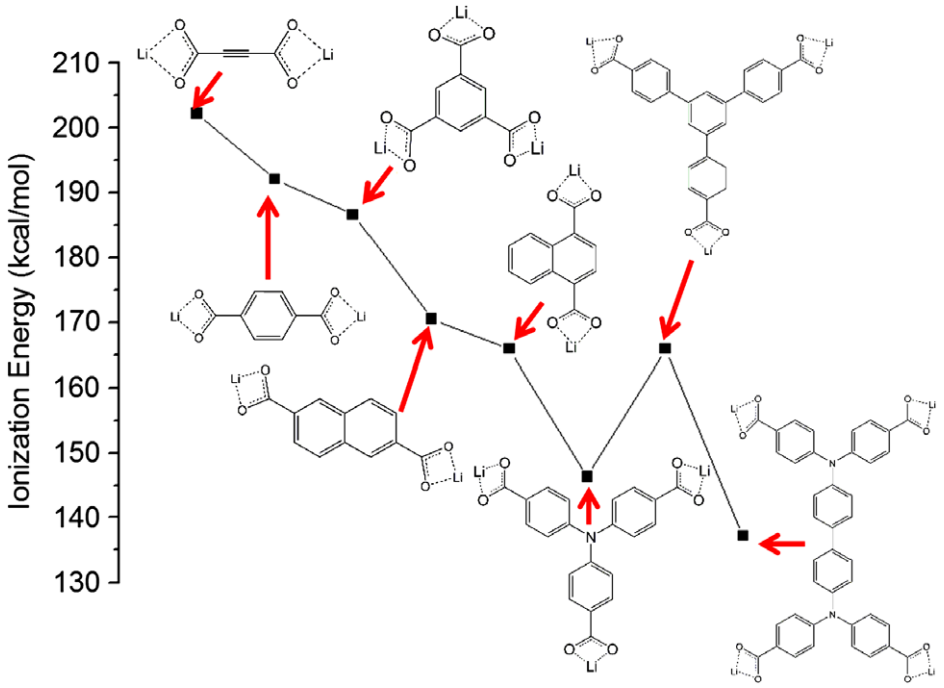

Figure 5. Ionization energies of representative organic linkers. (From left to right) Acetylenedicarboxylate (ADC), benzene-dicarboxylate (BDC), benzene-tricarboxylate (BTC), naphthalene-2,6-dicarboxylate (2,6-NDC), naphthalene-1,4-dicarboxylate (1,4-NDC), 4,4′,4″-nitrolotrisbenzonate (NTB), 1,3,5-benzene-tribenzoate (BTB), and *N*,*N*,*N*′,*N*′-tetrakis(4-carboxyphenyl)-biphenyl-4,4′-diamine (TCPDA), respectively.

groups leads to a decrease in the ionization energy in both types. This is because a positive charge can be delocalized to several phenyl groups. However, this tendency breaks for two types of organic linkers. The first case is where the ionization energy of NTB is lower than that of BTB. As NTB and BTB have three and four phenyl groups, respectively, one may expect that NTB should show higher ionization energy due to broken aromaticity of phenyl by a positive charge. In NTB, however, there is an additional lone pair from which the electron is more readily released. As a result, the organic linker containing a lone pair is more redox-active than others, implying that the MOFs with those organic linkers can participate in reduction reactions of transition-metal nanoparticles. The same rationale can be applied to another organic linker having lone pair, TCPDA.[40] The ionization energy of TCPDA is even lower than that of NTB because TCPDA has more phenyl groups.

Large organic linkers containing nitrogen could enhance hydrogen spillover. MOFs contain metal clusters in their structure, which takes a significant toll on the weight-percent capacity of hydrogen storage. In order to overcome this weakness, Ganz and Dornfeld proposed that huge organic linkers could offer more sites for hydrogen spillover.[34] We suggest that nitrogen-based large organic linkers can be the excellent hydrogen spillover acceptors. Even when the organic linker is huge with some connectors, hydrogenation will start easily and will smoothly propagate to another phenyl ring once the positive charge is established at the nitrogen atom. The present suggestion could be more effective and practical than other proposals involving defects at least in two points.[6] First, as we already mentioned, the defects in MOF are not good for the structural stability, while introducing a positive charge would not critically affect the geometry of the organic linker. The second point is that the huge organic linker can provide more sites for hydrogen spillover.

Conclusion

Through DFT calculations using a model of an MOF, we showed that NTB can be the receptors of hydrogen atoms to the point of full saturation of all sites on phenyl rings, suggesting that hydrogen spillover may happen for NTB. The initial hydrogenation has a large barrier for NTB, but the energy barrier is greatly reduced in the positively charged NTB. The successive hydrogenation is also facile for the charged NTB. The propagation of hydrogenation to the second and the third ring is easily done for the positively charged organic linker. The biggest barrier to spillover can be removed by having a positive charge on the organic linker. After being charged, NTB could be saturated exothermically not only on one ring but also on all rings. Saturation of one ring in NTB increases the binding energy of the first step of other rings because the electron-donating force is reduced as saturation progresses. It was also demonstrated that organic linkers with the nitrogen neighboring phenyls have lower ionization energies compared to other organic linkers consisting of only hydrocarbons. Accordingly,

we expect that a combination of nitrogen-based organic linkers and chemical doping of transition-metal particles can lead to the spillover with high efficiency. We propose MOFs containing nitrogen-based organic linkers with more phenyl groups as promising candidates for hydrogen storage system based on the hydrogen spillover.

Acknowledgments. The authors wish to thank Prof. A. J. Buglass for helpful advices. This work was supported by the Undergraduate Research Participate Program at KAIST, and by grants from the National Research Foundation (2010–0016243 and 2007–0056095) and KISTI (KSC-2011-C2-18).

References

1. A. J. Robell, E. V. Ballou, M. Boudart, *J. Phys. Chem.* **1964**, *68*, 2748.
2. L. Wang, R. T. Yang, *Energy Environ. Sci.* **2008**, *1*, 268.
3. L. Wang, R. T. Yang, *Cat. Rev.-Sci. Eng.* **2010**, *52*, 411.
4. P. Jena, *J. Phys. Chem. Lett.* **2011**, *2*, 206.
5. Y. H. Hu, L. Zhang, *Adv. Mater.* **2010**, *22*, E117.
6. K. Lee, Y.-H. Kim, Y. Y. Sun, D. West, Y. Zhao, Z. Chen, S. B. Zhang, *Phys. Rev. Lett.* **2010**, *104*, 236101.
7. S. S. Han, H. Kim, N. Park, *J. Phys. Chem. C* **2011**, *115*, 24696.
8. K.-S. Lin, A. K. Adhikari, K.-C. Chang, M.-T. Tu, W. Lu, *Catal. Today* **2011**, *164*, 23.
9. G. M. Psofogiannakis, T. A. Steriotis, A. B. Bourlinos, E. P. Kouvelos, G. C. Charalambopoulou, A. K. Stubos, G. E. Froudakis, *Nanoscale* **2011**, *3*, 933.
10. Y. Li, R. T. Yang, *J. Am. Chem. Soc.* **2005**, *128*, 726.
11. Y. E. Cheon, M. P. Suh, *Angew. Chem. Int. Ed.* **2009**, *48*, 2899.
12. Y. Li, R. T. Yang, *J. Am. Chem. Soc.* **2006**, *128*, 8136.
13. R. C. Lochan, M. Head-Gordon, *Phys. Chem. Chem. Phys.* **2006**, *8*, 1357.
14. A. J. Lachawiec, T. R. DiRaimondo, R. T. Yang, *Rev. Sci. Instrum.* **2008**, *79*, 063906.
15. A. J. Lachawiec, R. T. Yang, *Langmuir* **2008**, *24*, 6159.
16. Y. Li, F. H. Yang, R. T. Yang, *J. Phys. Chem. C* **2007**, *111*, 3405.
17. N. R. Stuckert, L. Wang, R. T. Yang, *Langmuir* **2010**, *26*, 11963.
18. S. S. Han, S.-H. Choi, A. C. T. van Duin, *Chem. Commun.* **2010**, *46*, 5713.
19. C.-H. Chen, C.-C. Huang, *Microporous Mesoporous Mater.* **2008**, *109*, 549.
20. P.-J. Tsai, C.-H. Yang, W.-C. Hsu, W.-T. Tsai, J.-K. Chang, *Int. J. Hydrogen Energy* **2012**, *37*, 6714.
21. C. I. Contescu, C. M. Brown, Y. Liu, V. V. Bhat, N. C. Gallego, *J. Phys. Chem. C* **2009**, *113*, 5886.
22. C.-S. Tsao, Y. Liu, H.-Y. Chuang, H.-H. Tseng, T.-Y. Chen, C.-H. Chen, M.-S. Yu, Q. Li, A. Lueking, S.-H. Chen, *J. Phys. Chem. Lett.* **2011**, *2*, 2322.
23. L. Wang, R. T. Yang, *J. Phys. Chem. C* **2008**, *112*, 12486.
24. A. C. Chien, S. S. C. Chuang, *Int. J. Hydrogen Energy* **2011**, *36*, 6022.
25. M. A. Miller, C.-Y. Wang, G. N. Merrill, *J. Phys. Chem. C* **2009**, *113*, 3222.
26. L. Wang, N. R. Stuckert, H. Chen, R. T. Yang, *J. Phys. Chem. C* **2011**, *115*, 4793.
27. S. Proch, J. Herrmannsdörfer, R. Kempe, C. Kern, A. Jess, *Chem. Eur. J.* **2008**, *14*, 8204.
28. M. Suri, M. Dornfeld, E. Ganz, *J. Chem. Phys.* **2009**, *131*, 174703.
29. G. M. Psofogiannakis, G. E. Froudakis, *J. Phys. Chem. C* **2009**, *113*, 14908.
30. I. López-Corral, E. Germán, M. A. Volpe, G. P. Brizuela, A. Juan, *Int. J. Hydrogen Energy* **2010**, *35*, 2377.
31. G. M. Psofogiannakis, G. E. Froudakis, *Chem. Commun.* **2011**, *47*, 7933.
32. G. M. Psofogiannakis, G. E. Froudakis, *J. Phys. Chem. C* **2011**, *115*, 4047.
33. A. K. Singh, M. A. Ribas, B. I. Yakobson, *ACS Nano* **2009**, *3*, 1657.
34. E. Ganz, M. Dornfeld, *J. Phys. Chem. C* **2012**, *116*, 3661.
35. H.-Y. Wu, X. Fan, J.-L. Kuo, W.-Q. Deng, *J. Phys. Chem. C* **2011**, *115*, 9241.
36. M. P. Suh, Y. E. Cheon, E. Y. Lee, *Chem. Eur. J.* **2007**, *13*, 4208.
37. P. Prins, *Chem. Rev.* **2012**, *112*, 2714.
38. M. J. Frisch, G. W. Trucks, H. B. Schlegel, G. E. Scuseria, M. A. Robb, J. R. Cheeseman, J. A. Montgomery Jr.. , T. Vreven, K. N. Kudin, J. C. Burant, J. M. Millam, S. S. Iyengar, J. Tomasi, V. Barone, B. Mennucci, M. Cossi, G. Scalmani, N. Rega, G. A. Petersson, H. Nakatsuji, M. Hada, M. Ehara, K. Toyota, R. Fukuda, J. Hasegawa, M. Ishida, T. Nakajima, Y. Honda, O. Kitao, H. Nakai, M. Klene, X. Li, J. E. Knox, H. P. Hratchian, J. B. Cross, V. Bakken, C. Adamo, J. Jaramillo, R. Gomperts, R. E. Stratmann, O. Yazyev, A. J. Austin, R. Cammi, C. Pomelli, J. W. Ochterski, P. Y. Ayala, K. Morokuma, G. A. Voth, P. Salvador, J. J. Dannenberg, V. G. Zakrzewski, S. Dapprich, A. D. Daniels, M. C. Strain, O. Farkas, D. K. Malick, A. D. Rabuck, K. Raghavachari, J. B. Foresman, J. V. Ortiz, Q. Cui, A. G. Baboul, S. Clifford, J. Cioslowski, B. B. Stefanov, G. Liu, A. Liashenko, P. Piskorz, I. Komaromi, R. L. Martin, D. J. Fox, T. Keith, M. A. Al-Laham, C. Y. Peng, A. Nanayakkara, M. Challacombe, P. M. W. Gill, B. Johnson, W. Chen, M. W. Wong, C. Gonzalez, J. A. Pople, *Gaussian 09, Revision C.02*, Gaussian, Inc., Wallingford, CT, 2009.
39. A. Mavrandonakis, W. Klopper, *J. Phys. Chem. C* **2008**, *112*, 3152.
40. Y. E. Cheon, J. Park, M. P. Suh, *Chem. Commun.* **2009**, *36*, 5436.

